

## Application of the Molecular Simulation Technique To Characterize the Structure and Properties of an Aromatic Polysulfone System. 2. Mechanical and Thermal Properties

Cun Feng Fan\*

Molecular Simulations, Inc., 796 North Pastoria Avenue, Sunnyvale, California 94086

Shaw Ling Hsu

Department of Polymer Science and Engineering, University of Massachusetts, Amherst, Massachusetts 01003

Received July 1, 1991; Revised Manuscript Received September 12, 1991

**ABSTRACT:** The structure of aromatic amorphous polysulfone was simulated and the energy and internal strain minimized by using molecular dynamics and mechanics methods developed earlier. A plot of the total potential energy as a function of volume or density indicates the existence of an optimum state possessing both the lowest energy and the least internal stress. The minimum-energy structure has a computed density of  $1.17 \pm 0.02 \text{ g/cm}^3$ , in good agreement with the experimental value. The mechanical and thermal properties of amorphous polysulfone were simulated using these model amorphous structures. The form of the stiffness matrix and the calculated associated elastic constants agree with known values for such an isotropic amorphous polymer. The thermal expansion coefficient calculated using molecular dynamics also agrees with the experimental value.

### Introduction

The prediction of macroscopic properties for amorphous materials based upon their microscopic structures is an extremely complex and difficult process. In contrast, the theoretical modulus of a crystalline polymer can be calculated with reasonable accuracy from known force constants associated with individual internal coordinates and the equilibrium crystalline structure.<sup>1-3</sup> An exact relationship between the molecular deformation behavior of crystalline polymers and their macroscopic properties can be obtained, and the calculated results may then be verified by diffraction or spectroscopic techniques.<sup>4-8</sup> Similar methods cannot be readily applied to amorphous polymer chains. An exact relationship between molecular geometric parameters and macroscopic deformation behavior cannot be established due to the disordered chain conformation distribution. Alternate methods need be developed which incorporate detailed information obtained from studies of the statics and dynamics of localized amorphous structures. Such studies can then be extended to obtain an understanding of the macroscopic behavior.

A number of studies have demonstrated the application of molecular simulation methods to calculated mechanical properties of polymers.<sup>9-13</sup> In some recent studies, an atomistic model was used to calculate macroscopic properties for amorphous polypropylene.<sup>11-13</sup> It was found that entropic contributions to the elastic deformation behavior can be neglected in polymeric glasses.<sup>12</sup> When this amorphous polymer is deformed, the vibrational contribution to the total internal energy change is only a few percent and can also be neglected. With these assumptions, the elastic constants were calculated from the second derivatives of the total potential energy change with respect to the overall strain of the system, and the calculated results agreed well with experimental data. The results of that study give considerable support to the idea that computer simulation of atomistic and molecular structures can lead to greater understanding of macroscopic behaviors or even predict macroscopic properties of amorphous polymeric materials.

A similar approach was used to obtain macroscopic properties of amorphous aromatic polysulfone, denoted PSF. In all instances, an accurate representation of the amorphous structure is necessary. In our previous study, model structures of amorphous aromatic PSF were simulated.<sup>14</sup> Structural information, such as long-range pair distribution functions or localized rotational barriers, was obtained. In this study, Theodorou and Suter's earlier work was modified in order to derive a procedure to relate macroscopic mechanical properties to a simulated structure. Even with extremely fast workstations, only polymers of at most several hundred atoms can be studied currently by the atomistic approach. It is necessary to determine whether the simulated structure is consistent with all characteristics associated with an amorphous state. In view of the large number of conformations, it is impractical to seek a global minimum. Nevertheless questions should be raised regarding whether the properties can in fact be derived for a structure close to, but not necessarily at, thermodynamic equilibrium. In this study, the elastic constants and thermal expansion coefficients for PSF have been calculated, and the accuracy of these calculations is considered.

### Simulation Technique

The monomeric repeating unit of the aromatic polysulfone, poly(oxy-1,4-phenylenesulfonyl-1,4-phenyleneoxy-1,4-phenyleneisopropylidene-1,4-phenylene), is shown in Figure 1. The practical size of the polymer studied is 10 chemical repeats. Due to the large size of the monomer unit, the size of the polymer studied is considerable. A previous study showed that the chain length chosen is sufficient for generating an effectively isotropic amorphous system. The computer program used is a commercial material simulation package, POLYGRAF, by Molecular Simulations, Inc. The force field used in the POLYGRAF molecular mechanics and dynamics calculations has been previously described.<sup>15</sup>

The bulk amorphous state is simulated through use of periodic boundary conditions; i.e. a polymer chain is packed into a cubic cell, and the cell is infinitely repeated in three-

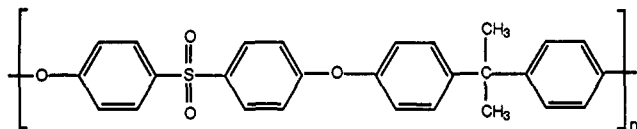


Figure 1. Chemical structure of aromatic polysulfone.

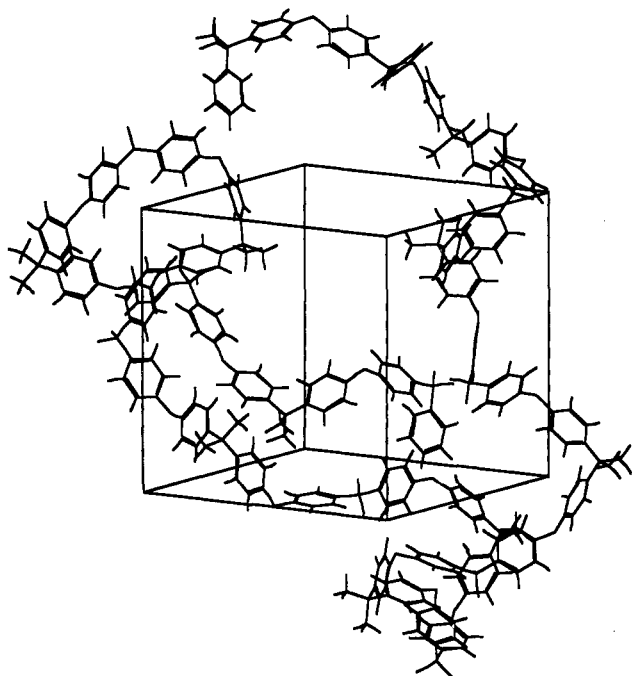


Figure 2. Model structure of amorphous aromatic polysulfone.

dimensional space. Details regarding the procedure and parameters used in constructing the model amorphous structure were presented previously.<sup>14</sup> The initial structures generated through the amorphous builder are usually in a highly energetic state, primarily because of the overlap of van der Waals' radii allowed in the building process for effective packing of the polymer chain into the cell with specified density. The total potential energy of the model structure is then minimized by alternately using molecular mechanics and molecular dynamics. The constant-pressure molecular dynamics algorithm used in POLYGRAF is similar to that proposed by Nose and Klein.<sup>16</sup> This approach is based on earlier studies by Andersen,<sup>17</sup> as well as other studies by Parrinello and Rahman.<sup>18-20</sup> The cell mass  $W$  is chosen as the total mass of the atoms in the simulated unit cell. Cell shape is kept fixed during the minimization procedure. The initial cell density was taken to be 1.20 g/cm<sup>3</sup>. The optimum density of the system is then calculated. The cubic shape of the motif greatly simplifies calculation of elastic constants. Figure 2 presents one of the 10 structures used in our analysis. This structure illustrates only the parent chain and associated cell which, due to the periodic boundary condition, is surrounded by 26 similar cells.

## Results and Discussion

When a polymer chain is packed into a cubic cell under periodic boundary conditions, the density of the polymer must be specified. Generally the experimental value at a particular temperature is used.<sup>10</sup> In this fashion the temperature dependence is indirectly incorporated. This approach raises a number of issues including the following:

(1) the structure obtained usually has a high internal stress, indicating the system is far from equilibrium; (2) the potential energy change upon deformation is inconsistent with the strain energy change. The potential energy

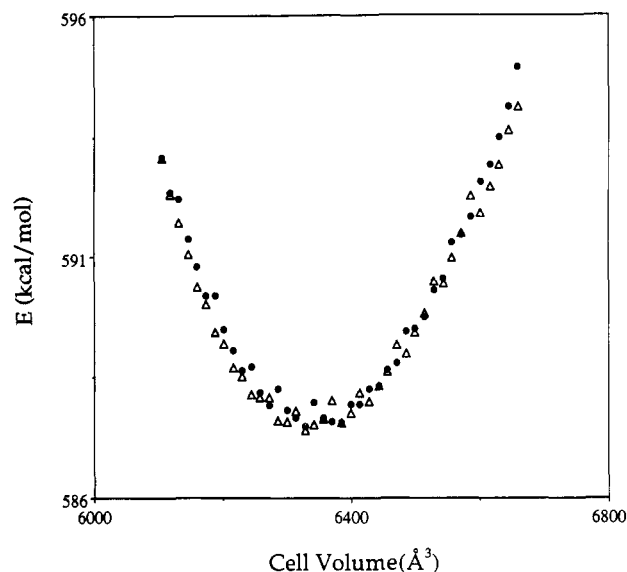


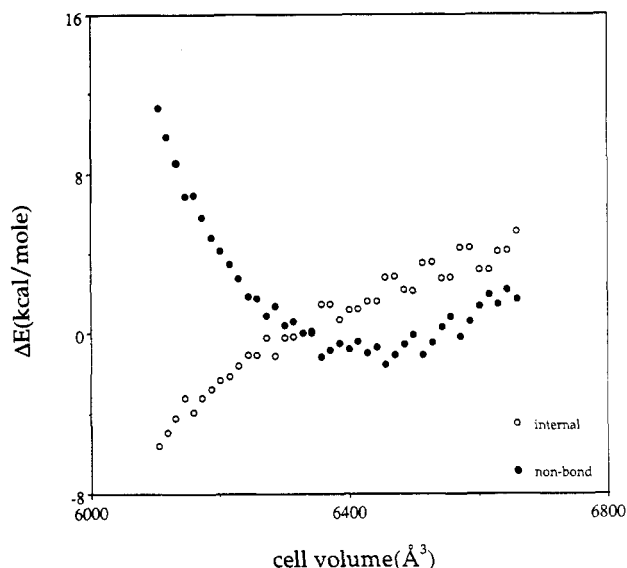
Figure 3. Potential energy of model PSF as a function of cell volume: (Δ) changes in energy when the initial state is being stretched; (●) changes in energy when the deformed structure is being compressed back to the initial state.

Table I  
Diagonal Terms of the Internal Stress Tensors (MPa) of Three Structures under Different Stress States

	stress free	tension	compression
$xx$	-18	287	-202
$yy$	5	275	-301
$zz$	-43	258	-351

of a model system decreases<sup>10</sup> under compression, while, by convention, the strain energy of the system should increase under tension or compression because external work is performed on the system during deformation. This inconsistency occurs because the assumed density for the amorphous structure is not the optimum value.

Our earlier study demonstrated that the density of the system can be obtained by relaxing cell parameters ( $A$ ,  $B$ ,  $C$ ,  $\alpha$ ,  $\beta$ ,  $\gamma$ ) in the minimization process. The predicted density ( $1.17 \pm 0.02$  g/cm<sup>3</sup>) is slightly lower than the experimental value ( $1.24 \pm 0.04$  g/cm<sup>3</sup>). In this study, the optimum structure of the system is obtained by calculating the potential energy of the system as a function of the cell size or, equivalently, under deformation, while maintaining the cubic cell shape. The initial structure with a density of 1.20 g/cm<sup>3</sup> is not a state with the lowest energy nor is it stress free. We have calculated the change in energy when this initial structure is stretched and then compressed back to the initial state. Changes in energy associated with stretching and compression are shown in Figure 3. The optimum structure is one with minimum energy, as shown in this figure. In principle, the internal stress, the first derivative of the potential energy with respect to strain, of the structure with the minimum potential energy should be zero. The internal stress in the simulated structure could not be completely eliminated, particularly for the model with the cell kept at cubic shape during the energy minimization process. The diagonal terms of the internal stress tensor, which can be related directly to system stress, are listed in Table I for three structures (one near the minimum of the potential energy curve shown in Figure 3, one at the far right, and one at the far left). The structures that depart from the potential energy minimum are either under tension or compression. If mechanical deformation is performed for the two representative stressed structures, changes in the potential energy and strain energy will be inconsistent.



**Figure 4.** Bonded and nonbonded energies of model PSF as a function of cell volume.

The structure with the lowest potential energy corresponds to the stress-free structure. The total energy consists of contributions from intra- (bond, angle, torsion, etc.) and intermolecular contributions (mainly van der Waals interaction). For the state characterized by the minimum in total energy, the nonbonded term has its minimum value, while the intramolecular component does not. The monotonic increase of the intramolecular term as a function of cell size in the strain range studied indicates that, in order to pack the polymer chain into the cell under the periodic condition, the bonds and bond angles, as well as torsional angles, of the model polymer are distorted. The energy minimization procedure takes contributions from bonded and nonbonded components into consideration in order to seek the global minimum. From the relative contributions shown in Figure 4, the potential energy increase is due solely to the contribution from repulsive nonbonded interactions when this structure is compressed.

The total potential energy change as a function of strain, virtually identical for compression or extension, is expected. Irreversible deformation can occur, even for a small strain. Such behavior is shown in Figure 5. When a high-density sample placed in a small cell volume is stretched, the potential energy as a function of strain may exhibit discontinuities. Following the procedure used to obtain the data shown in Figure 3, we have stretched an initial structure and then compressed it back to the initial state. In this case, energy change upon compression follows a normal continuous curve. For the simulated amorphous polymer, the total potential energy surface contains a large number of local minima. The energy minimization process brings the system to one of these minima. The barrier between structures may not be high and in fact can be quite low. The final structure represents only one of many similar structures. When the polymer is deformed, changes in the structure may force the system to seek an alternate local minimum. As there are no significant differences among the structures, treating a transformation from one to another represented by discontinuous jumps in energy change, shown in Figure 5 as plastic deformation, would be inappropriate.

Calculation of elastic constants associated with an amorphous polymer can be performed by utilizing several methods. The simplest and most straightforward technique is to apply a unidirectional external load to the unit

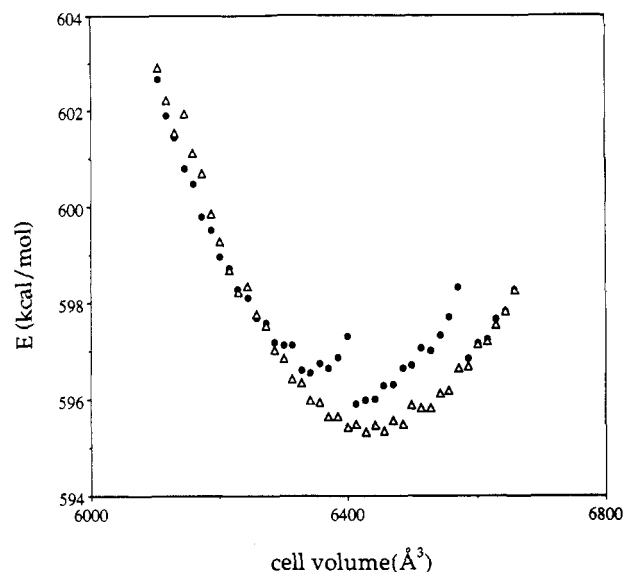


**Figure 5.** Potential energy of model PSF as a function of cell volume (irreversible changes): (●) changes in energy when the initial state is being stretched; (Δ) changes in energy when the deformed structure is being compressed back to the initial state.

cell and then minimize the energy under constant stress. Elastic constants can be obtained from the ratio of the applied stress to the resultant dimensional changes. The average value obtained for the three principal directions would be used to characterize the amorphous polymer. The major problem associated with this approach is that the undeformed cubic unit cell may not be the ideal shape. Using periodic conditions, the simulated amorphous structure is generally associated with a triclinic cell with three different cell lengths,  $A$ ,  $B$ ,  $C$ , and three different angles,  $\alpha$ ,  $\beta$ ,  $\gamma$ . For simplification, a cubic cell has been used in these simulations. If the cell parameters are released during the minimization procedure, the dimensional changes corresponding to the applied stress are determined by two factors, external stress and perhaps a slight shape change. For small stress values, shrinkage or expansion in the lateral direction may be observed due to the second factor. Although large stress could be applied to alleviate this effect, the results obtained would be unreliable due to the possibility of transformation from one local minimum to another, as discussed above. If an irregular cell shape is used for both undeformed and deformed states, calculation of the stiffness matrix is difficult and tedious.

Theodorou and Suter found that the entropic contribution to an elastic response can be neglected in polymeric glasses.<sup>10</sup> The vibrational-transition contribution to the total internal energy change is only a few percent and can be neglected as well. It has been found that the conclusion obtained by Theodorou and Suter may not be true for all polymers.<sup>21-23</sup> The existing data are not precise enough to permit a definitive conclusion concerning the importance of entropic contribution associated with the bulk deformation of polymeric glass. Theodorou and Suter's assumption is justifiable in molecular mechanics or energy minimization. Their structure is effectively simulated at 0 K since no kinetic energy or temperature effect is directly considered. Entropic contribution to the elastic deformation process of polymeric glass vanishes at 0 K.

The elastic constants can be obtained from changes in the total potential energy of structures subjected to deformation under these assumptions. The stiffness matrix completely describes the elastic properties of a material and can be computed in two different ways. After an initial energy minimization, a second energy minimi-

zation is performed under a small fixed strain. Changes in energy and in internal stress are then calculated. By definition, the first derivative of the potential energy with respect to strain is the internal stress tensor and the second derivative represents the stiffness matrix. The derivatives can be estimated from a three-point finite difference equation. In the energy method

$$C_{ii} = (\partial^2 U / \partial \epsilon_i^2) / V \\ = (U_+ + U_- - 2U_0) / (V \epsilon_i) \quad (1)$$

where  $U$  is the total energy,  $V$  is the volume,  $\epsilon_i$  is the component  $i$  of the strain tensor,  $U_+$  is the minimized energy under tension,  $U_-$  is that under compression, and  $U_0$  is the energy of the undeformed structure. In the energy method only the diagonal terms of the stiffness matrix can be calculated accurately because of significant errors involved in evaluation of second derivatives by the finite difference method. In the stress method the stiffness matrix is given by

$$C_{ij} = (\partial^2 U / \partial \epsilon_i \partial \epsilon_j) / V \\ = \partial \sigma_i / \partial \epsilon_j \\ = (\sigma_{i+} - \sigma_{i-}) / (2\epsilon_j) \quad (2)$$

where  $\sigma_i$  is the  $i$ th component of the internal stress tensor.  $\sigma_{i+}$  and  $\sigma_{i-}$  are the components associated with the stress tensor under tension and compression, respectively. The advantage of this method is that only the first derivative need be evaluated numerically since internal stress can be calculated in the minimization process.<sup>14</sup> This method also yields the entire stiffness matrix. Only eq 2 is used to calculate the elastic constants of amorphous polymers. Usually a very small strain (0.05%) is applied to the structure incrementally 12 times, i.e. from  $\pm \epsilon_1$  to  $\pm \epsilon_6$ . The stiffness matrix is then calculated by following changes in each component of the internal stress tensor at each strain.

The entire stiffness matrix obtained by averaging 10 structures (GPa) is

$$C_{ij} = \begin{pmatrix} 5.13 & 2.03 & 2.45 & -0.04 & 0.07 & -0.16 \\ 1.79 & 5.13 & 1.70 & -0.35 & -0.03 & 0.80 \\ 1.86 & 1.76 & 5.23 & 0.18 & -0.62 & -0.27 \\ -0.02 & -0.04 & 0.00 & 1.71 & -0.27 & -0.42 \\ -0.36 & -0.26 & -0.25 & -0.57 & 1.76 & -0.52 \\ -0.71 & -0.17 & -0.03 & -0.16 & -0.62 & 1.34 \end{pmatrix} \quad (3)$$

This matrix is to be compared to the idealistic matrix associated with a totally isotropic amorphous state<sup>24</sup>

$$C_{ij} = \begin{pmatrix} \lambda + 2\mu & \lambda & \lambda & 0 & 0 & 0 \\ \lambda & \lambda + 2\mu & \lambda & 0 & 0 & 0 \\ \lambda & \lambda & \lambda + 2\mu & 0 & 0 & 0 \\ 0 & 0 & 0 & \mu & 0 & 0 \\ 0 & 0 & 0 & 0 & \mu & 0 \\ 0 & 0 & 0 & 0 & 0 & \mu \end{pmatrix} \quad (4)$$

where  $\lambda$  and  $\mu$  are Lamé constants. For isotropic amorphous material, the stiffness matrix should be symmetric; i.e.  $C_{ij} = C_{ji}$ . However, as shown in eq 2, the actual calculation of  $C_{ij}$  and  $C_{ji}$  follows two different deformation histories. Therefore, the calculation departs from the idealistic case. Nevertheless, it is clear that the calculated stiffness matrix for the model amorphous aromatic polysulfone demonstrates the basic features of an isotropic material. The mechanical properties in the three principal directions are very close. The elements which should be zero for ideal isotropic materials are significantly smaller in comparison to the diagonal values. In molecular simulation experiments, although the periodic boundary

Table II  
Calculated Elastic Constants of Model Aromatic Polysulfone

Lamé constant, $\lambda$	$1.96 \pm 1.48$ GPa
Lamé constant, $\mu$	$1.60 \pm 0.65$ GPa
Young's modulus, $E$	$3.88 \pm 1.51$ GPa
bulk modulus, $B$	$3.02 \pm 1.48$ GPa
Poisson's ratio, $\nu$	$0.24 \pm 0.15$

condition simulates bulk properties, calculated results for a cell containing 540 atoms may not be sufficient. It is virtually impossible to achieve the macroscopic isotropy required by eq 4 for the ideal case. If the sample size is increased, better results can be obtained. However, accurate measured values exist for very few samples.

The Lamé constants for the model structures can be calculated from eq 3 by using the diagonal elements.

$$\lambda = 1/3(C_{11} + C_{22} + C_{33}) - 2/3(C_{44} + C_{55} + C_{66})$$

$$\mu = 1/3(C_{44} + C_{55} + C_{66}) \quad (5)$$

Other elastic constants can be derived from  $\lambda$  and  $\mu$ .<sup>24</sup> The calculated results and their standard deviations are listed in Table II. The calculated Young's modulus is slightly higher than the experimental value,  $\sim 2.6$  GPa.<sup>25</sup> This difference may result from the fact that the calculation represents an ideal interaction between atoms or molecules, while interaction in the actual material may be weakened by voids and other structural defects. Molecular simulation provides the upper limit of the elastical constants. A major concern regarding this calculation is that Poisson's ratios obtained are unexpectedly small. For most glassy polymers, Poisson's ratios are in the range of 0.33–0.38.<sup>26</sup> In comparison to the earlier study on atactic polypropylene, the errors are quite large. Considering the complexity of the PSF monomer unit, however, the results obtained in this calculation are acceptable.

In molecular simulation, thermal expansion coefficients can generally be calculated by different approaches, such as the static method and, more directly, the method of molecular dynamics. In the static method, the thermal expansion coefficient,  $\alpha$ , can be obtained from the following thermodynamic expression relating the thermal expansion coefficient to bulk compressibility, internal pressure, and temperature

$$\alpha = \text{Tr}(\sigma) / (3TB) + P/TB \quad (6)$$

where  $\text{Tr}(\sigma)$  is the internal stress tensor trace,  $B$  is the bulk modulus,  $P$  is the pressure (usually 1 atm), and  $T$  is the temperature in kelvin. The static model may provide a reasonable result if the temperature corresponding to the simulated static structure is known. However, as the nature of the energy minimization or molecular mechanics excludes any temperature effect, the temperature of the structure has to be indirectly incorporated by specifying the density of the model structure, usually using experimental data. Therefore this method cannot predict the thermal expansion coefficient without specific knowledge of material property. If the molecular simulation technique is used to design new materials, the static method alone is insufficient. Furthermore, if the model structure must match experimental density at a particular temperature, the structure may be forced into a stressed state, as discussed earlier. This stressed state is characterized by the fact that the potential energy change upon deformation is inconsistent with the strain energy and the internal stress tensor is not close to zero. The sign of the internal stress tensor depends on the value of the assigned experimental density, whether positive (or negative) or

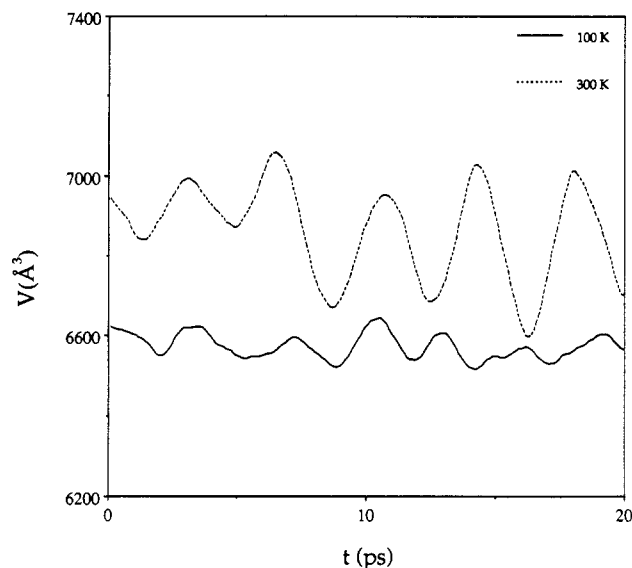


Figure 6. Volume fluctuation of model PSF at two different temperatures.

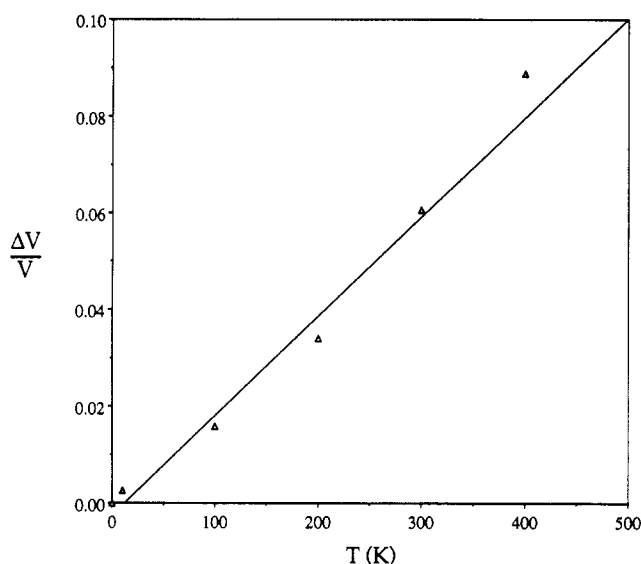


Figure 7. Volume changes of model PSF as a function of temperature.

lower (or higher) than the density calculated using the simulation technique. In the static model, the cell size change in Figure 3 is regarded as a result from temperature change rather than external strain. The right part of the curve is explained as the energy change as temperature increases from 0 K. The physical meaning of the left part of the curve is insignificant.

In this study a direct approach or molecular dynamics method was used to calculate the thermal expansion coefficient. In this dynamic method, the system is simulated with molecular dynamics at constant temperature. The volume of the system will fluctuate as a function of time. For a sufficiently long period, a reasonable average of the volume at a particular temperature can be obtained. Simulations can be performed at several different temperatures, and the slope of the volume change as a function of time will yield the thermal expansion coefficient. In addition to the overall thermal expansion coefficient, molecular dynamics also provides information regarding the relative flexibility of various parts of the polymer structure. Figure 6 shows the volume fluctuation as a function of time at two different temperatures. Each point in the curves is the average volume of 100 steps of the microcanonical dynamics with each step of 0.001 ps. After 100

steps the temperature is calculated from the average kinetic energy. The calculated temperature is compared to the bath temperature. If the difference is larger than the specified temperature window (50 K), the velocities are scaled to ensure the new velocities will correspond to the bath temperature. Both average volume and volume fluctuation increase with temperature. At 300 K the volume fluctuation is about 1.7%, while at 100 K the volume fluctuation is less than 0.5%. Figure 7 shows the volume change relative to 0 K as a function of temperature. The 0 K volume is obtained from the minimum in Figure 3. A good linear fit indicates the system behaves well in molecular dynamics. The volume thermal expansion coefficient obtained from the slope of Figure 7 is  $2.16 \times 10^{-4} \text{ K}^{-1}$ . The linear thermal expansion coefficient is one-third the volume expansion coefficient ( $7.2 \times 10^{-5} \text{ K}^{-1}$ ), which agrees well with the experimental value ( $5.5 \times 10^{-5} \text{ K}^{-1}$ ).<sup>25</sup>

## Conclusions

An atomistic model structure is generated to study mechanical and thermal properties. The optimum structure with lowest energy as well as internal stress can be obtained through a simulated hydrostatic deformation process. The calculated elastic constants from the structure predict the upper limit of the elastic moduli of the material, while the thermal expansion coefficient agrees very well with experimental data. This modeling of macroscopic properties of aromatic amorphous polysulfone through molecular mechanics and molecular dynamics convincingly demonstrates the applicability of atomistic and molecular simulation to the study of amorphous polymers, even polymers with complicated monomer structures.

**Acknowledgment.** We acknowledge Dr. Tahir Cagin, who contributed to this work.

## References and Notes

- (1) Tashiro, K.; Kobayashi, M.; Tadokoro, H. *Macromolecules* **1977**, *10*, 413.
- (2) Tashiro, K.; Kobayashi, M.; Tadokoro, H. *Macromolecules* **1978**, *11*, 908.
- (3) Tashiro, K.; Kobayashi, M.; Tadokoro, H. *Macromolecules* **1978**, *11*, 914.
- (4) Dulmage, W. J.; Contois, L. E. *J. Polym. Sci.* **1958**, *28*, 275.
- (5) Schaufele, R. J.; Shimanouchi, T. *J. Chem. Phys.* **1967**, *47*, 3605.
- (6) Sakurada, I.; Kaji, K. *J. Polym. Sci., Part C* **1970**, *31*, 57.
- (7) Holiday, L.; White, J. W. *Pure Appl. Chem.* **1971**, *26*, 545.
- (8) Hsu, S. L.; Krimm, S. *J. Appl. Phys.* **1977**, *48*, 4013.
- (9) Boyd, R.; Pant, P. V. K. *Macromolecules* **1991**, *24*, 4073.
- (10) Boyd, R.; Pant, P. V. K. *Macromolecules* **1991**, *24*, 4078.
- (11) Theodorou, D. N.; Suter, U. W. *Macromolecules* **1985**, *18*, 1467.
- (12) Theodorou, D. N.; Suter, U. W. *Macromolecules* **1986**, *19*, 139.
- (13) Theodorou, D. N.; Suter, U. W. *Macromolecules* **1986**, *19*, 379.
- (14) Fan, C. F.; Hsu, S. L. *Macromolecules*, in press.
- (15) Mayo, S. L.; Olafson, B. D.; Goddard, W. A., III. *J. Phys. Chem.* **1990**, *94*, 8897.
- (16) Nose, S.; Klein, M. L. *Mol. Phys.* **1983**, *50*, 1055.
- (17) Andersen, H. C. *J. Chem. Phys.* **1980**, *72*, 2384.
- (18) Parrinello, M.; Rahman, A. *Phys. Rev. Lett.* **1980**, *45*, 1196.
- (19) Parrinello, M.; Rahman, A. *J. Appl. Phys.* **1981**, *52*, 7182.
- (20) Parrinello, M.; Rahman, A. *J. Chem. Phys.* **1982**, *76*, 2662.
- (21) Matheson, R. *Macromolecules* **1987**, *20*, 1847.
- (22) Matheson, R. *Macromolecules* **1987**, *20*, 1851.
- (23) Matheson, R. *J. Phys. Chem.* **1987**, *91*, 6062.
- (24) Malvern, L. E. *Introduction to The Mechanics of A Continuous Medium*; Prentice-Hall: Englewood Cliffs, NJ, 1969.
- (25) Margolis, J. M. *Engineering Thermoplastics*; Marcel Dekker: New York, 1985.
- (26) *Modern Plastics Encyclopedia*; Wiley-Interscience: New York, 1975.

**Registry No.**  $(-\text{OC}_6\text{H}_4-p-\text{SO}_2\text{C}_6\text{H}_4-p-\text{OC}_6\text{H}_4-p-\text{C}(\text{Me})_2-\text{C}_6\text{H}_4-p-)_n$  (SRU), 25135-51-7.